Annals of Nuclear Energy 214 (2025) 111220

Contents lists available at ScienceDirect

Annals of Nuclear Energy

journal homepage: www.elsevier.com/locate/anucene

KFK iron sphere neutron and gamma benchmark sensitivity/uncertainty analysis to n/γ nuclear data and potential use for cross section improvement

I. Kodeli *

UKAEA, Culham Centre for Fusion Energy Abingdon, OX14 3DB, United Kingdom

ARTICLE INFO

Keywords:
Gamma-ray
Benchmark experiments
Shielding
Sensitivity-uncertainty analysis
Nuclear data

ABSTRACT

The SUSD3D computer code has been recently updated with new features including the extension of the nuclear data sensitivity and uncertainty (S/U) analysis to gamma-ray quantities such as gamma flux and heating. Gamma relevant nuclear data (ENDF material files MF16, MF23, MF26) can be processed allowing S/U of coupled neutron/gamma problems. The code is available from the NEA data Bank as part of the new version of the XSUN-2023 computer code package which includes also the latest updates of the cross section and covariance matrix libraries based on the JEFF-3.3, ENDF/B-VIII.0 and FENDL-3.2 evaluations. The code was applied to the S/U analysis of the KFK neutron and γ-ray leakage benchmark to evaluate the sensitivities to iron neutron and gamma cross sections.

Sensitivity of neutron and gamma flux to the iron inelastic, elastic and capture cross sections was found to depend in an interesting way on iron shell thickness, even changing from positive to negative, which suggests that these type of measurements (in particular if repeated using more modern measurement techniques) can be powerful for the validation of iron cross sections in the high energy ranges. The need for the evaluation of gamma-ray covariances is raised.

1. Introduction

Nuclear data sensitivity and uncertainty of neutron flux and the related quantities are commonly used today and provide a good means to understand the performance and identify the weaknesses of nuclear data files. Gamma fluxes were to some extent neglected. However, just like neutrons, gamma radiation emerging from neutron reactions with materials or from radioactive decay poses radiation protection hazards in nuclear reactors linked to gamma heating, nuclear damage or photo-nuclear reactions. An accurate estimation of gamma-ray intensity and spectra, together with the associated uncertainties, is therefore important for fission and fusion reactor applications.

Notable sources of gamma-rays include gammas produced as a result of reactions with neutrons:

- Radioactive decay of unstable isotopes (secondary gammas)
- gamma radiation accompanying nuclear reactions of fission (prompt gammas), capture, inelastic scattering.

Gamma-rays interact with matter (mostly electrons) through:

- photo-effect (absorption)
- incoherent scattering (e.g. Compton effect)
- pair production (absorption)
- coherent (elastic) scattering of gamma-rays by bound electrons
- interaction with the nucleus: photo-neutron (γ,n) reaction

With a few exceptions (e.g. (γ,n) reactions) most reactions take place with electrons, therefore for most general purposes the gamma nuclear data can be organised as elemental data sets instead of isotope specific as is the case for neutrons. In radiation transport codes the gamma-rays are in general treated as “down-scattering” from neutron energy groups.

In the ENDF nuclear data files, the sections MF = 23 to MF = 27 are reserved for photo-atomic interaction data. The uncertainties in the calculated gamma spectra may be in some cases relatively high comparing to neutron spectra. However, the nuclear data sensitivity and uncertainty analyses are not commonly performed. A possible reason for this neglect is the lack of the corresponding covariance data for gamma-

* Corresponding author.
E-mail address: Ivan.kodeli@ukaea.uk.

https://doi.org/10.1016/j.anucene.2025.111220
Received 1 November 2024; Received in revised form 7 January 2025; Accepted 17 January 2025
Available online 30 January 2025

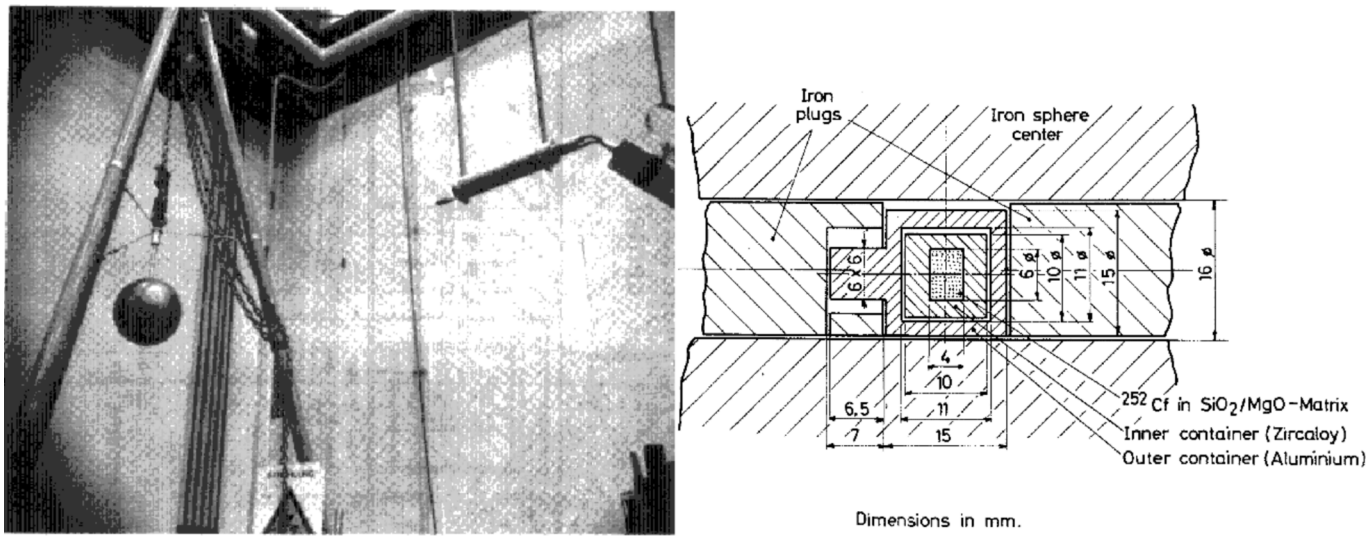

Fig. 1. KFK iron sphere with the proton recoil detector and the neutron source model. The ^{252}Cf is stored in a SiO_2 cylinder at the centre of the source (figures taken from the SINBAD (Kodeli and Sartori, 2021) evaluation of KFK benchmark).

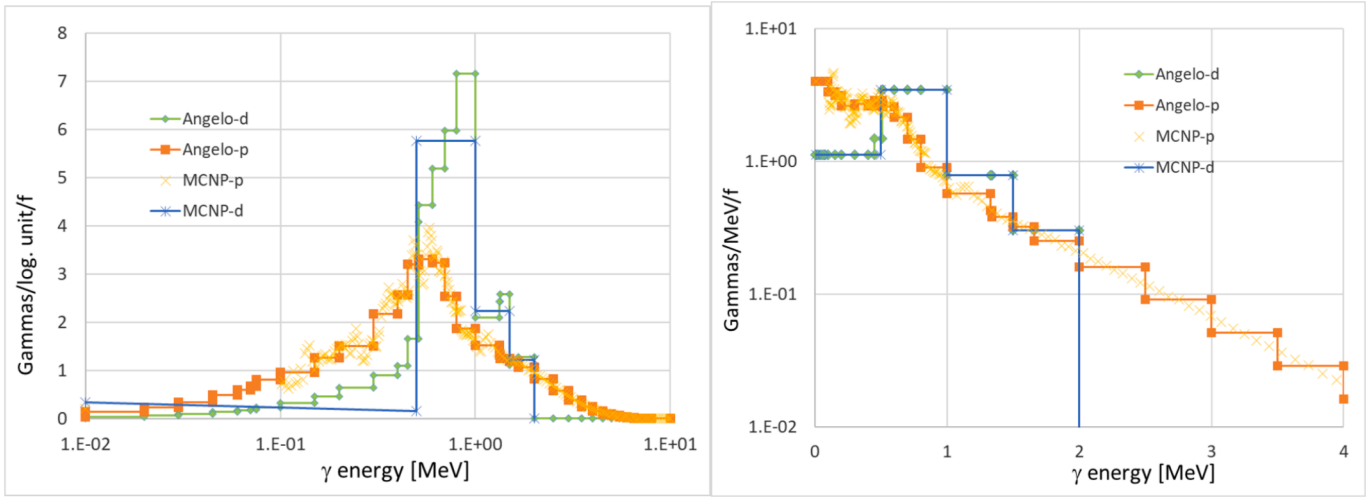

Fig. 2. Prompt and delayed fission gamma spectra (PFGS/DFGS) of ^{252}Cf presented in log and linear energy scale: Angelo-p and Angelo-d correspond respectively to the PFGS and DFGS interpolated using the Angelo code. MCNP-p and MCNP-d correspond to the spectra included in the MCNP input in the new SINBAD evaluation.

ray interactions.

2. Extensions of the SUSD3D perturbation code

To fill the above gap regarding the S/U analysis, the SUSD3D code (Kodeli, 2023; Kodeli and Slavič, 2017; Kodeli, 2001) was extended to cover the sensitivity analysis of the gamma related quantities. A preliminary verification was performed using the KFK gamma-ray benchmark.

SUSD3D (Kodeli, 2023; Kodeli and Slavič, 2017; Kodeli, 2001) is a multi-dimensional nuclear cross-section sensitivity and uncertainty code suitable for complex multidimensional neutral particle transport studies. Sensitivity coefficients and standard deviations in nuclear parameters of interest (k_{eff}, β_{eff}, reaction rates, neutron/gamma flux) due to input cross section data and their uncertainties are calculated based on the first-order generalised perturbation theory (GPT). Relative sensitivity profile $S_g^{x,k}$ expresses the fractional change of an integral response R (such as reaction rate, heating rate or flux), per fractional variation of a cross section for reaction x in a particular nuclide k, and energy group g ($\sigma_g^{k,x}$):

$$S_g^{x,k} = \frac{1}{R}\,\frac{\partial R}{\partial \sigma_g^{x,k} / \sigma_g^{x,k}} \tag{1}$$

Using GPT the relative sensitivity is calculated from the following expression (Kodeli, 2001):

$$S_g^{k,x} = \frac{1}{R}\sum_i \Delta V_i \left[\rho_i^x \left(-\sigma_g^{k,x} \sum_m \Phi_{g,i,m}\cdot\Phi^*_{g,i,m}\cdot\Delta\Omega_m + \sum_{g'}\sum_{l=0}^{L}\sigma_{l,g\to g'}^{k,x}\sum_{n=-l}^{l} M_{g,i}^{l,n}\cdot M_{g',i}^{*l,n}\right) + \sigma_{g,i}^{Dk,x}\sum_m \Phi_{g,i,m}\cdot\Delta\Omega_m\right]$$

where:

$\Phi_{g,i,m}\cdot\Phi^*_{g,i,m}$ = direct and adjoint angular (neutron/gamma) flux in energy group g, space interval i and angular interval m.

$M_{g,i}^{l,n}\cdot M_{g',i}^{*l,n}$ = direct and adjoint flux moments, corresponding to the space interval i and energy group g.

$\sigma_g^{k,x}$ = microscopic cross section for reaction x in nuclide k, in group g.

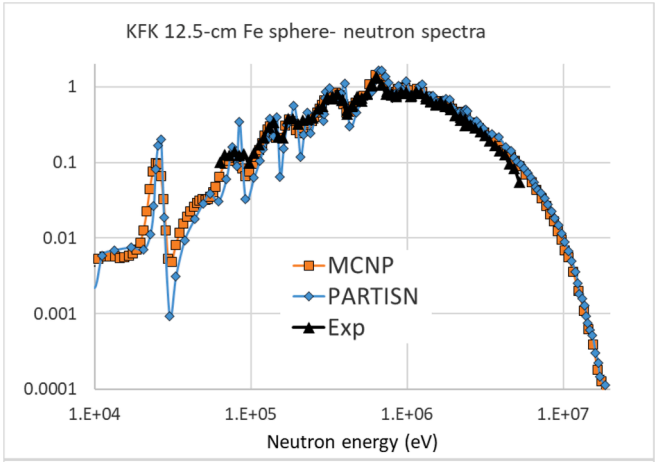

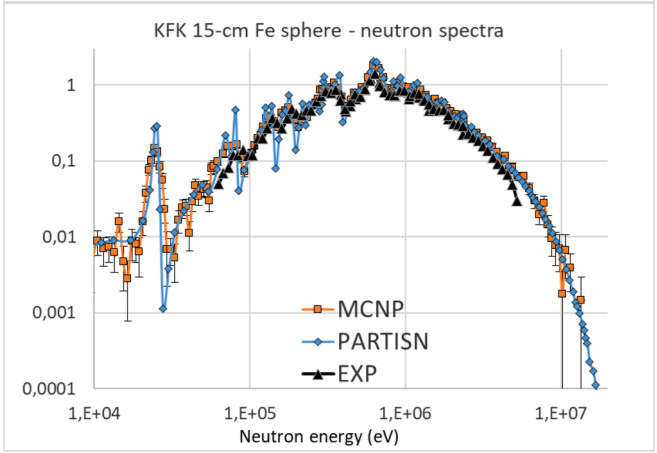

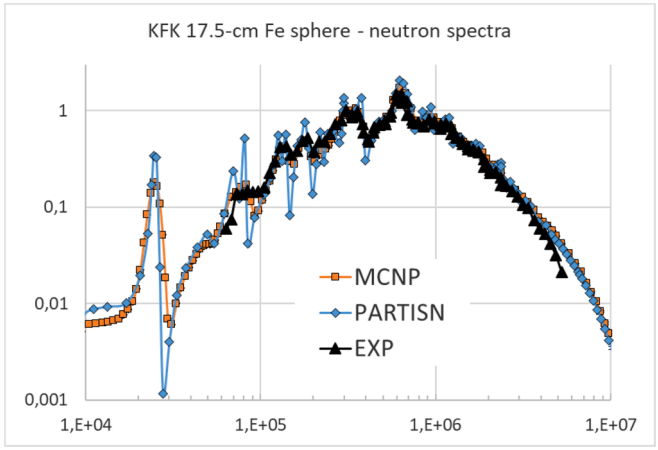

Fig. 3. KFK iron sphere Comparison between the measured neutron spectra and those calculated using the MCNP and PARTISN codes (Ø25 to Ø35-cm spheres). Nuclear cross section data were taken from the FENDL-3.2 library.

$\sigma_{l,g\to g'}^{k,x}$ = l'th Legendre moment of the microscopic scattering cross section from group g to g', for reaction x in isotope k.

$\sigma_{g,i}^{Dk,x}$ = detector response function (source for adjoint calculation).

ΔV_i = volume of the space interval i.

$\Delta\Omega_m$ = angular interval m.

ρ_i^x = atomic number density of nuclide k in space interval i.

The new version of the SUSD3D code can process gamma-ray relevant nuclear data thus allowing for the analysis of coupled n/γ problems to evaluate the sensitivity of the gamma-ray quantities such as gamma flux and heating to neutron and gamma nuclear data. SUSD3D code covers the sensitivity to different cross-section types: neutron gain term (MF = 3), neutron loss term (MF = 6), direct term (sensitivity to neutron/gamma response function) (MF = 2), secondary angular (SAD − MF = 4), and energy distributions (SED − MF = 5), gamma production (MF16), gamma loss and gain terms (MF23, MF26). In the same way as for the neutron responses, the normalisation of the sensitivities to units %/% is done internally in the code if requested using the option "resp = -1". Sensitivities are normalised to the integral response R defined in "sens 22" or "sens 32" (contrary to "sens 2" or "sens 12" used for the neutron part).

Several types of uncertainties can be thus considered, i.e. those due to neutron multi-group cross sections, energy-dependent response functions, secondary angular (SAD) or energy distribution (SED) uncertainties. Constrained and unconstrained methods are available for the SED (e.g. prompt fission neutron spectra), and mu-bar (P_1 Legendre term) as well as higher P_N terms can be taken into account. The particle transport calculations are done externally using the existing discrete ordinates (S_N) codes such as DOORS, DANTSYS, PARTISN, and the calculated direct and adjoint fluxes are passed to the SUSD3D code via the flux moment files. The sensitivity profiles are folded with the cross-section covariance matrices to determine the variance of an integral response of interest. However, a complete uncertainty analysis for gamma flux is at present not possible due to the lack of covariance data corresponding to gamma-ray nuclear data.

The latest version of the SUSD3D code is available as part of the XSUN-2023, computer code package released through the NEA Data Bank. XSUN code package (Kodeli, 2023) is a user–computer interface environment developed to simplify the execution, pre- and post-processing of the input and output data for a complete and self-consistent set of deterministic codes. The package integrates the codes TRANSX-2 (MacFarlane, 1995), PARTISN (Alcouffe et al., 2008), and SUSD3D (Kodeli, 2001), all available from the OECD/NEA Data Bank and RSICC. XSUN-2023 is the 3rd released version, after XSUN-2013 and −2017. The package includes multigroup cross section and covariance matrix libraries based on the JEFF-3.3 (Plompen et al., 2020), ENDF/B-VIII.0 (Brown et al., 2018) and FENDL-3.2 (Fusion Evaluated Nuclear Data Library - FENDL-3.2b, xxxx) evaluations for up to 440 nuclides, depending on the nuclear data library.

Among the above cross-sections, the FENDL-3.2 library with 211 neutron/42 gamma groups is suitable for coupled neutron/gamma S/U analysis. On the other hand, the FENDL-3.2 library includes covariance data for only a limited number of isotopes (58), and no covariances relative to the gamma nuclear data. Several format inconsistencies and errors were found and corrected in the multigroup gamma-ray processed files, which is probably due to a limited use and testing of these data in the past.

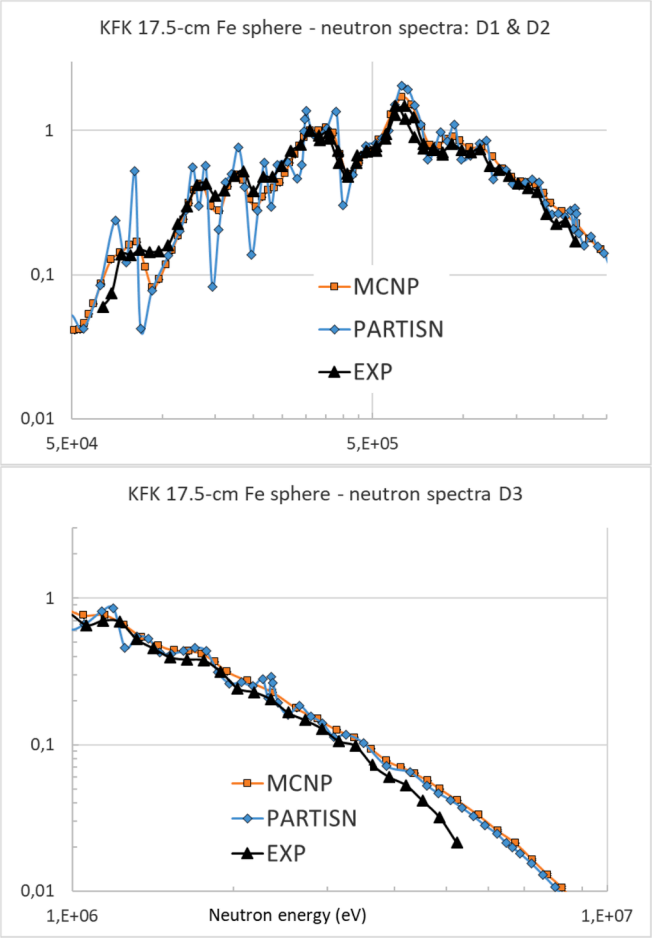

Fig. 4. A detailed comparison between the calculated and measured neutron spectra for proton recoil spectrometers (detectors D1, D2) and He-3 spectrometer (D3). FENDL-3.2 nuclear data were used in the MCNP and PARTISN calculations.

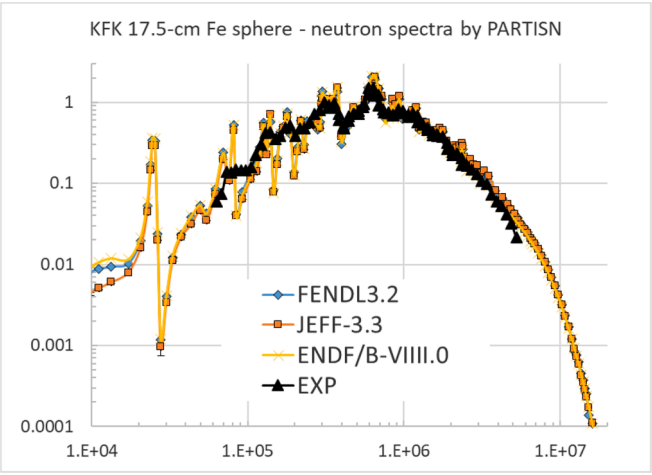

Fig. 5. Comparison between the measured and calculated neutron spectra using different nuclear data libraries: FENDL-3.2, JEFF-3.3 and ENDF/B-VIII.0. All spectra were calculated using the PARTISN code.

3. Application to sinbad kfk gamma leakage benchmark

Despite the importance of gamma radiation in reactor applications, relatively few gamma-ray benchmarks are included in the SINBAD shielding benchmark database and the uncertainty involved in gamma transport calculations (and the discrepancy between the calculated and measured results) is often relatively high. Some of the gamma-ray measurements available in SINBAD (Kodeli and Sartori, 2021) are listed below:

•RFNC-Photon Leakage Spectra from Al, Ti, Fe, Cu, Zr, Pb, ^{238}U Spheres.

•RFNC Photon Spectra from H_2O, SiO_2 and NaCl.

•ASPIS Neutron/Gamma-Ray Transport Through Water/Steel Arrays.

•SB2 CSEWG Secondary Gamma-Ray Production Cross Sections.

•SB3 CSEWG Secondary Gamma-Ray Production Cross Sections (1969).

•ORNL Photon Skyshine Experiment Benchmark.

•OKTAVIANs.

•Several FNG and FNS benchmarks.

In addition to the above benchmarks, the SINBAD evaluation of KFK-1977 measured gamma spectra from Ø25, 30 and 35 cm Fe spheres using a bare ^{252}Cf(s.f.) source (Jiang and Werle, 1977; Jiang and Werle, 1978; Jiang and Werle, 1977; Werle et al., 1975) was proposed and prepared by Stanislav Simakov (Simakov and Fischer, 2022) in the scope of the OECD Working Parties on Evaluation Cooperation Subgroup 47 (WPEC SG47) (Kodeli, 2023) activities. The new evaluation was discussed within the SINBAD Task Force activities and will be released in SINBAD. The evaluation includes a detailed description of the facility, the measurement methods, the experimental gamma spectra with uncertainties and MCNP models. This will complement the existing KFK Iron sphere SINBAD evaluation which is limited to the neutron leakage spectra.

KFK-1977 benchmarks consisted of neutron and gamma-ray leakage spectra measurements from a set of high-purity iron spheres (C 0.07 %, Mn 0.05 %, P 0.009 %, S 0.007 %) of diameters up to 40 cm (up to 35 cm for gammas) with a ^{252}Cf source in the centre (Fig. 1). Measurements were performed at Forschungszentrum Karlsruhe (former KFK) around 1975 – 1977 and are reported in (Jiang and Werle, 1977; Jiang and Werle, 1978; Jiang and Werle, 1977; Werle et al., 1975). The neutron spectra measured using the proton recoil and ^{3}He spectrometers from a set of iron spheres of various diameters (15, 20, 25, 30, 35, and 40 cm) were included in SINBAD already in the early 1990′s (Werle et al., 1975).

To reduce the background the experimental arrangement was located in a hall, at a distance of at least 2 m from the ground and more than 3 m from the nearest walls. Three sets of gas-filled proton recoil spectrometers with diameters 4.8 and 8.9 mm and effective lengths of 12.6 and 83.5 mm, and a ^{3}He spectrometer were used for neutron spectra measurements. The statistical uncertainties were between 5–10 % and systematic uncertainties 8–11 % for the proton recoil and 5–6 % for the ^{3}He spectrometers. SPEC-4 code was used for spectra unfolding. Neutron energy spectra from 60 keV to 5 MeV, and from 100 keV to 8 MeV were measured using the proton recoil and He-3 spectrometers, respectively. Neutron source strength uncertainty was ± 5 %.

Several deficiencies of the neutron spectra measurements were identified by Simakov (Simakov and Fischer, 2018):

– probable typos in the reported neutron spectrum of bare Cf source, with contradicting values reported in different publications,

– shadow bar used to measure background was too thin to completely shield fast neutrons, allowing about 1 – 8 % of high energy neutrons with energies 0.05–5 MeV to penetrate.

Absolute gamma-rays in the energy range between 300 keV and 3 MeV were measured with the Si(Li) Compton spectrometer positioned on the outer surface of the iron shells. The measurement uncertainties were around 10–20 %, including the response function uncertainties (~ 10 %) and statistical uncertainties (5–10 %). Due to the neutron background effects the authors of the experiment recommended to restrict

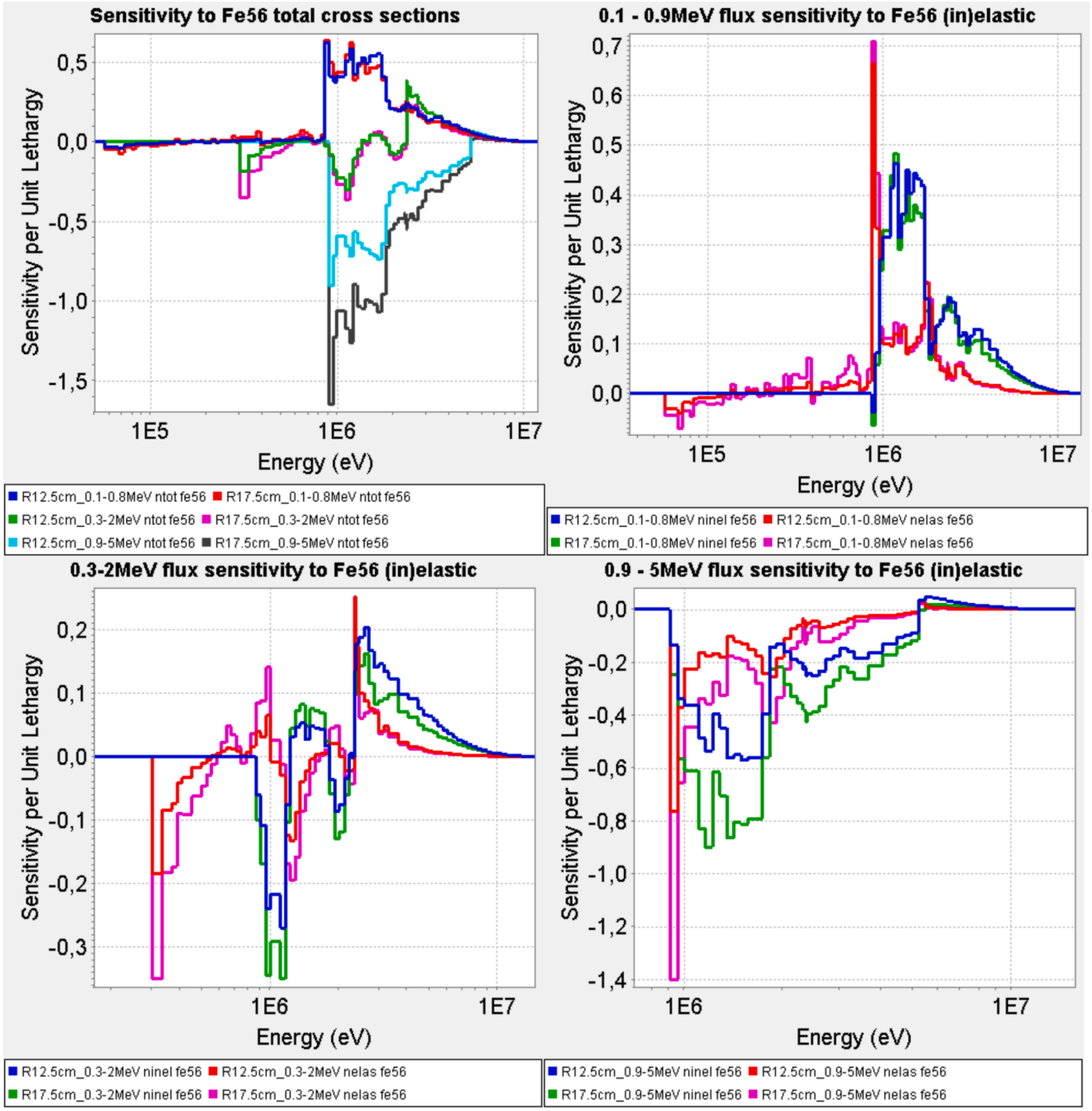

Fig. 6. Sensitivity of the neutron flux integrated over three energy ranges (0.1–0.9 MeV, 0.3–2 MeV and 1–5 MeV) to the ^{56}Fe total, inelastic and elastic neutron cross sections for iron spheres with the radii of 12.5 and 17.5 cm.

Table 1
Uncertainty in the neutron flux of different energy ranges due to ^{56}Fe cross section uncertainties.

Detector (energy range)	12.5 cm JEFF3.3	17.5 cm JEFF3.3	ENDF/B-VIII.0	FENDL-3.2
D1 (0.1 – 0.8 MeV)	1.5 %	1.5 %	1.7 %	0.5 %
D2 (0.3 – 2 MeV	0.6 %	0.7 %	0.7 %	0.6 %
D3 (0.9 – 5 MeV	1.8 %	3.0 %	4.3 %	1.0 %

the use of experimental data to the 0.5 – 2 MeV energy range.

In the SPEC-4 unfolding procedure used to unfold gamma-ray spectra from the measured Compton electron energy, the contribution of high energy gammas (>3 MeV) was neglected, which may result in errors of 10 % and 20 % at energies between 1 and 2 MeV (see (Simakov and Fischer, 2022) for more details).

^{252}Cf emits both neutrons and gammas. Whereas the ^{252}Cf spontaneous prompt fission neutron spectrum (PFNS) is considered as a neutron standard and is thus a suitable neutron source for nuclear data measurements, the number and spectra of prompt and delayed fission gammas (PFGS/DFGS) are less well characterised. The prompt and delayed components of the ^{252}Cf gamma source are studied in (Simakov

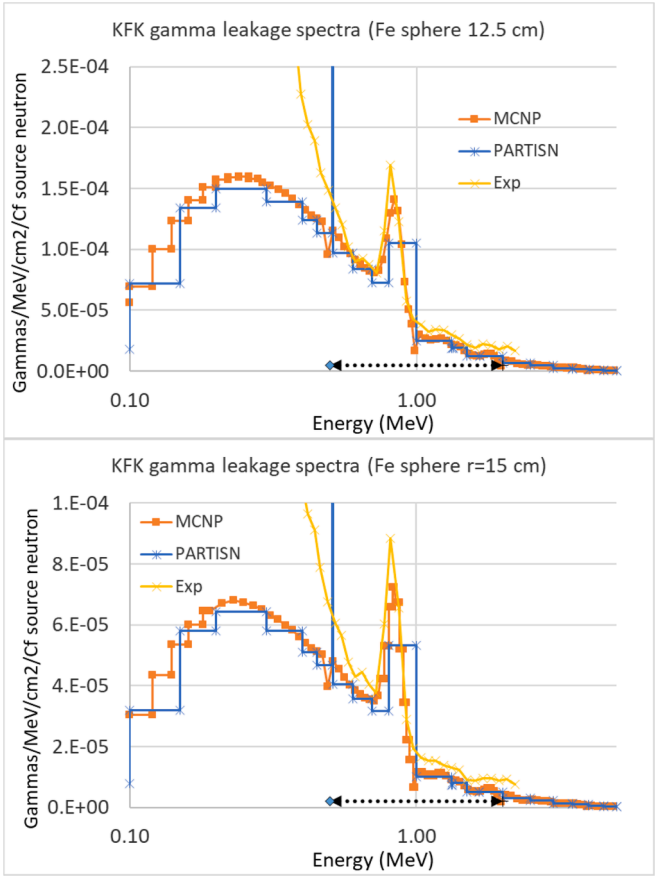

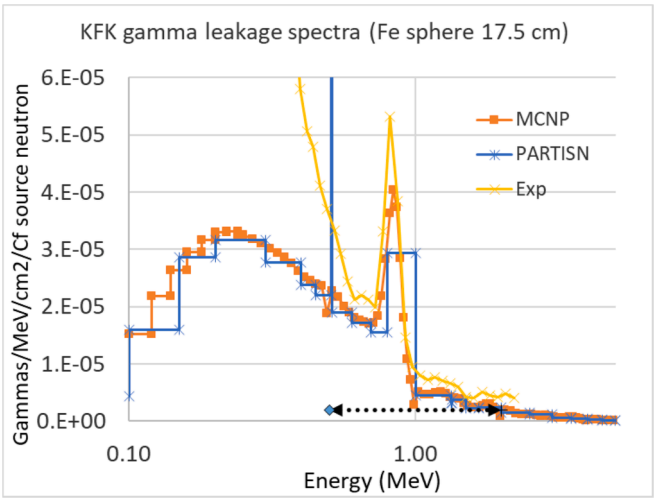

Fig. 7. Comparison between the measured gamma spectra and those calculated using the MCNP and PARTISN codes. Note that electrons were not transported in MCNP, which explains the difference in the missing 511 keV annihilation γ-rays observed in PARTISN assuming gamma emission in place e^+ are generated. Nuclear data were taken from the FENDL-3.2 library.

and Fischer, 2022; Simakov, 2024). For the present study the ^{252}Cf neutron and gamma source spectra provided in the MCNP inputs of the SINBAD compilation by S. Simakov (Simakov and Fischer, 2022) were used. Considerable spread among the experimental data as well as evaluated gamma source spectra is reported in (Simakov and Fischer, 2022; Simakov, 2024). As the neutron and gamma source spectra in the MCNP input are provided in different energy group structures, they were converted into the 211 neutron and 42 gamma groups of the multigroup FENDL-3.2 library using the ANGELO computer code (Kodeli, 2008) using a simple stepwise interpolation, linear in energy. The comparison of the original and the interpolated spectra is shown in Fig. 2, both in logarithmic and linear energy scale. The distortion within the interpolated group is due to the presentation in log energy scale (i.e. the division by $\log(E_{upper}/E_{lower})$).

3.1. *Transport and nuclear data sensitivity/uncertainty analysis −neutron spectra*

The three Ø25, 30 and 35 cm-diameter Fe spheres were calculated using the tools available in the XSUN-2023 package. Multigroup self-shielded cross sections were prepared by the updated TRANSX-2 code using the FENDL-3.2 211-neutron/42-gamma group cross section library available from the IAEA webpage (Fusion Evaluated Nuclear Data Library - FENDL-3.2b, xxxx). Direct and adjoint n/γ transport calculations were performed using the PARTISN code. Thus calculated neutron and γ fluxes were then used in the SUSD3D code to evaluate the sensitivity of the gamma flux to the underlying neutron and gamma cross sections.

The PARTISN neutron and gamma-ray spectra calculations were verified against the stochastic MCNP calculations using the model provided in (Simakov and Fischer, 2022), considered as reference since avoiding the inherent approximations of the deterministic transport codes (such as the use of multigroup cross sections, space mash discretisation). Comparisons between neutron spectra calculated using the PARTISN and MCNP codes, both based on the FENDL-3.2 nuclear data, are presented in Fig. 3. A more detailed zoom of the 17.5 cm radius sphere spectra, separately for the recoil and ^{3}He spectrometer measurements, is shown in Fig. 4. A very good agreement was observed in neutron spectra calculated using the PARTISN and MCNP codes, in particular above the energy of 1 MeV (Fig. 4). Some differences at lower energies may be attributed to the fact that resolution broadening was applied in the MCNP calculations, but not in PARTISN. S. Simakov estimated the experimental relative energy resolution of Si(Li) spectrometer to be (20——7)% in the gamma-ray energy range (0.5——3) MeV (Simakov and Fischer, 2022).

Fig. 5 compares the measured spectra for the 17.5-cm sphere with those calculated using the PARTISN code and different recent nuclear data libraries (FENDL-3.2, JEFF-3.3 and ENDF/B-VIII.0). Agreement between the calculated and measured spectra is reasonably good, with calculation overpredicting the high energy flux above ~ 1 MeV. The overprediction is large compared to the differences observed between calculations using different neutron cross section evaluations (JEFF-3.3, ENDF/B-VIII.0, −VIIII.1, FENDL-3.2). The overprediction is in contradiction with some more recent measurements (Rez sphere measurements, IPPE). Furthermore, at this high energy range above ~ 1 MeV the ENDF/B-VIII.0 based results seem to be in a better agreement with the experiment, which is also in contradiction with the results of most other iron benchmark experiments. These discrepancies are likely to be caused by the permeability of the shadow bar for fast neutrons as suggested in

Table 2
KFK benchmark: contribution of neutron-induced gammas and ^{252}Cf gamma source terms to the total, 0.5—2 MeV and 1—2 MeV gamma flux in the detector for the spheres of different radii.

Total γ	^{252}Cf neutron			^{252}Cf gammas		
Sphere radius (cm)	Total	Prompt	Delayed	Total	Prompt	Delayed
12.5	48.16 %	48.15 %	0.01 %	51.84 %	25.18 %	26.66 %
15	61.84 %	61.82 %	0.02 %	38.16 %	20.04 %	18.12 %
17.5	80.72 %	80.68	0.03 %	19.28 %	11.23 %	8.06 %
γ (0.5—2 MeV)	^{252}Cf neutron			^{252}Cf gammas		
Sphere radius (cm)	Total	Prompt	Delayed	Total	Prompt	Delayed
12.5	50.94 %	50.93 %	0.01 %	49.06 %	23.44 %	25.63 %
15	63.54 %	63.53 %	0.01 %	36.46 %	17.56 %	18.12 %
17.5	82.72 %	82.70 %	0.02 %	17.28 %	10.10 %	7.18 %
γ (1—2 MeV)	^{252}Cf neutron			^{252}Cf gammas		
Sphere radius (cm)	Total	Prompt	Delayed	Total	Prompt	Delayed
12.5	35.04 %	35.03 %	0.01 %	64.96 %	36.80 %	28.16 %
15	44.83 %	44.82 %	0.01 %	55.17 %	33.13 %	22.04 %
17.5	64.80 %	64.78 %	0.02 %	35.20 %	22.86 %	12.34 %

Table 3
Uncertainty in the 0.5 to 2 MeV gamma flux due to the uncertainty in ^{252}Cf PFNS and prompt and delayed gamma source spectra.

γ (0.5—2 MeV)	^{252}Cf neutron	^{252}Cf gammas	
Sphere radius (cm)	Prompt	Prompt	Delayed
12.5	6.6 %	6.1 %	4.5 %
15	8.0 %	5.0 %	3.3 %
17.5	9.5 %	2.7 %	1.4 %

(Simakov and Fischer, 2018). Comparison with other measurements using more accurate experimental techniques is needed to independently verify and clarify the differences observed (Simakov and Fischer, 2018).

Some specific trends can be observed in the sensitivities of neutron spectra to (iron) cross sections. Interestingly, as shown in Fig. 6 and Table 1, the sensitivity of the gamma flux with energy below ~ 1 MeV to the total iron cross section is very similar for the small and the large iron spheres. Increasing the radius of the spheres (from 12.5 to 17.5 cm) has therefore relatively small impact on the nuclear data related sensitivity and uncertainty of the neutron flux below 1 MeV. On the other hand, the sensitivity of high neutron enegy flux to iron inelastic (and elastic) cross sections increases considerably and the corresponding uncertainty doubles in value for the 35-cm vs. the 25-cm diameter sphere. Note that the uncertainties in the considered energy ranges are small due to the broad energy ranges used in this comparison and the cancellations involved. The uncertainty in neutron spectra at smaller energy intervals is larger and therefore using a finer energy mash instead of the three broad groups would of course lead to higher uncertainties.

Analysing the C/E trends for different energy intervals could therefore provide information on nuclear data deficiencies in the specific energy ranges and reactions. For example, for high neutron energy flux > 1 MeV a deteriorating C/E ratios with sphere thickness would indicate probable errors in the inelastic or/and elastic cross sections. On the other hand, observing C/E discrepances at lower energies could be a sign of an inconsistent repartition between the elastic and inelastic levels in the evaluated library (note from Fig. 6b and 6c that although the sensitivities to the total ^{56}Fe cross section are similar for all three spheres, some compensating variations with sphere thickness can be observed in the trends of sensitivities of the neutron flux < 1 MeV to the elastic and inelastic cross sections).

3.2. *Transport and nuclear data sensitivity/uncertainty analysis – Gamma spectra*

Just like for neutrons, the gamma flux in three (Ø25, 30 and 35 cm-diameter) Fe spheres was calculated using the FENDL-3.2 211-neutron/42-gamma cross section library available from the IAEA webpage (Fusion Evaluated Nuclear Data Library - FENDL-3.2b, xxxx). Fig. 7 compares the measured and the calculated gamma spectra demonstrating good agreement between MCNP and PARTISN is good, except the group around the 0.511 MeV positron annihilation peak, which can be explained by the fact that MCNP calculations did not include electron transport. Note that the low energy spectra may not be accurate due to the neglect of electron transport. Note that at high gamma energies around ~ 1 MeV the FENDL 42-group grid is quite broad, with only 3 energy groups between 0.7 and 1.33 MeV, compared to 19 groups for the MCNP calculations, which clearly have impact on the level of details observed both due to transport and Cf gamma source description.

S/U analysis of the gamma flux was performed using the SUSD3D code as explained in Chapter 2. Several types of computational uncertainties were considered, including the uncertainty in the neutron and gamma source distributions and in the nuclear cross sections.

The contribution P of the neutron-induced gammas, and ^{252}Cf prompt and delayed gammas to the gamma spectra at the detector position for different spheres and gammas of different energies was evaluated using the adjoint neutron and gamma fluxes calculated by the PARTISN code:

$$P_g^x = \sum_g \Phi_{g,i}^* \cdot \chi_g \cdot \Delta V_i \quad (2)$$

where $\Phi_{g,i}^*$ is the neutron/gamma adjoint flux in (neutron or gamma) energy group g, calculated using the adjoint source defined as either total, (0.5 – 2) MeV or (1 – 2) MeV gamma flux placed at the fission source position i.

χ_g is the fission spectrum (respectively neutron, gamma, prompt, delayed).

ΔV_i is the volume of the interval i.

As shown in Table 2, the contribution of neutron-induced gammas (i.e. from Fe(n,xγ) reactions) varies with gamma energy and increases with an increasing sphere radius from ~ 40 % to ~ 80 %.

The uncertainty in the gamma flux of energy between 0.5 to 2 MeV due to the uncertainty in PFNS and prompt and delayed gamma source spectra of ^{252}Cf was calculated using the constrained sensitivity method as coded in the SUSD3D code. The sensitivities derived from the adjoint neutron and gamma fluxes are defined in Eq. (2). The covariance matrices for the ^{252}Cf PFNS were taken from the ENDF/B-VIII.0 evaluation. Covariances for the ^{252}Cf prompt and delayed gamma source spectra are not readily available, therefore an (ad-hoc) uncertainty of 20 % was assumed, block-wise anti-correlated below and above the average gamma source energies. The resulting uncertainties are given in Table 3, and amount to up to ~ 10 % due to the PFNS (increasing with increasing sphere size). On the other hand, the uncertainties due to the ^{252}Cf prompt and delayed gamma source, roughly of a similar order of magnitude, tend to reduce with increased radius. Note however that the 20 % uncertainty in the ^{252}Cf gamma source is a very rough estimation based on the dispersion of the measured data and may underestimated in particular for the DFGS component, which is rather poorly studied (Kodeli, 2008). In addition, γ-ray spectrum of ^{252}Cf depends on the

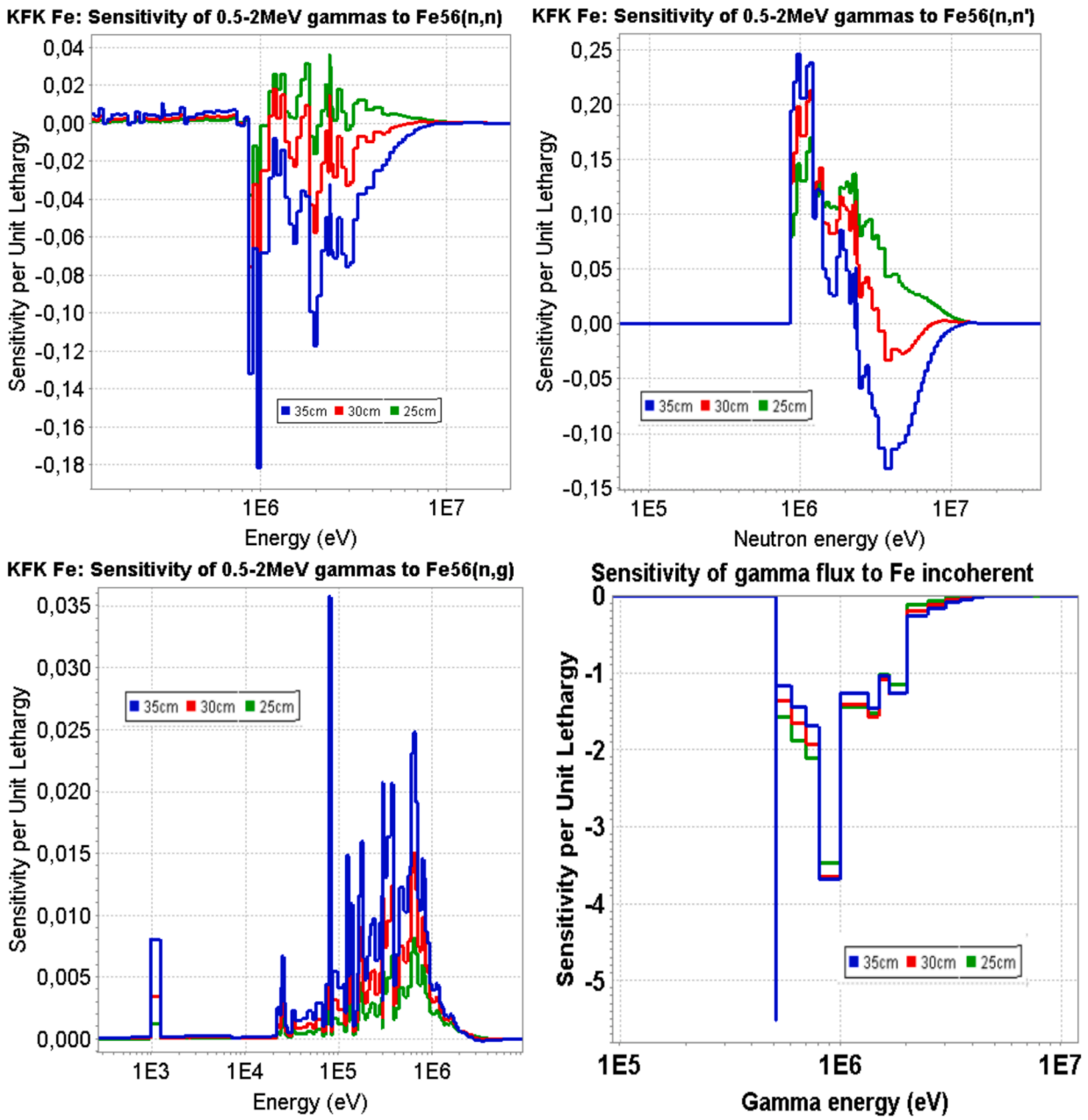

Fig. 8. Sensitivity of gamma flux between 0.51——2 MeV at detector position (radius 16.3——16.8 cm) to neutron elastic and inelastic scattering, neutron capture and photon incoherent (Compton) scattering cross sections for the iron spheres with the diameters between 25 and 35 cm.

purity and the age of the ^{252}Cf source (fission product accumulated, relative abundances of Cf isotopes).

Note that the Table 3 uncertainties only take into account the uncertainty in fission spectra, but not the uncertainty in gamma yield per fission. If/when available the impact of this uncertainty can be readily propagated to gamma flux uncertainty using the gamma source relative contributions presented in Table 2.

Examples of sensitivity profiles of the gamma flux between 0.5 and 2 MeV and the total gamma flux to the underlying nuclear data for the different iron spheres are shown on Figs. 8 and 9, respectively. Of particular interest is the decrease of the flux sensitivity to inelastic and elastic ^{56}Fe cross sections with increasing sphere radius. Both sensitivities, positive for the 25 cm-sphere, become negative for the 35-cm diameter sphere. This can be explained by the neutron spectra effects. Increase of (in)elastic cross section increases gamma flux production for small spheres, but also leads to gamma flux reduction through the retroactive neutron flux reduction for larger spheres.

The above can be exploited for the interpretation of the observed C/E trends, in particular for the validation of the ^{56}Fe inelastic cross sections at the high energy range. A shift from C/E over to underprediction (or vice versa) if observed would be a clear sign of the deficiencies in (in) elastic cross section data, provided that the other uncertainties, including experimental, are well controlled and understood.

4. Conclusions

The SUSD3D nuclear data perturbation code was extended to sensitivity and uncertainty analysis of gamma related quantities such as gamma flux and heating. The code, together with the 211-neutron/42-gamma group nuclear data from the FENDL-3.2 library was used to analyse the KFK neutron and γ-ray leakage iron sphere benchmark. The analysis revealed very interesting features in the sensitivity profiles of

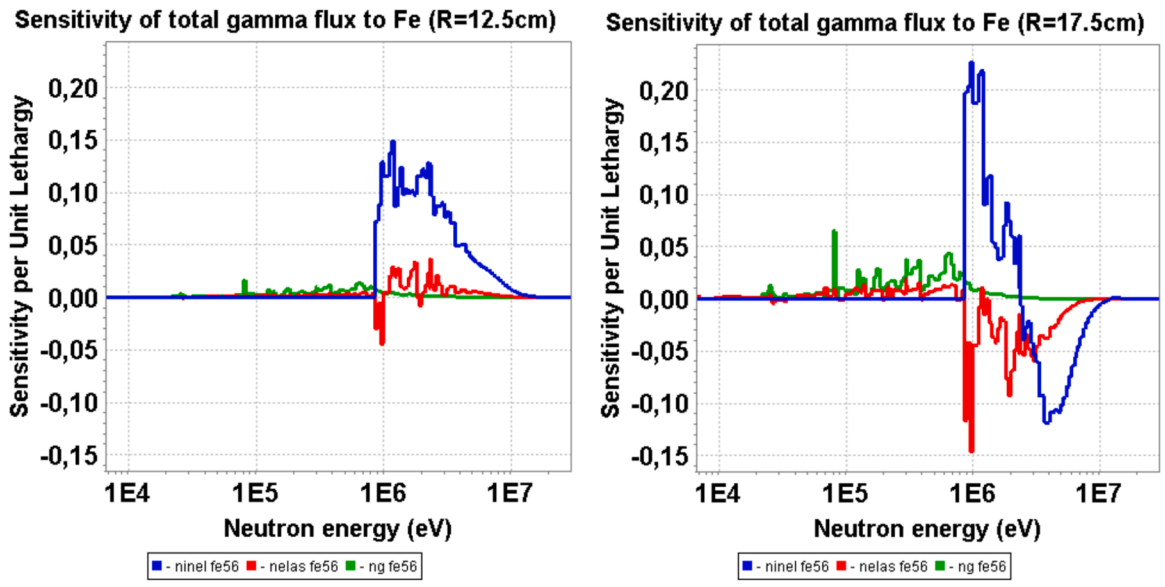

Fig. 9. Sensitivity of the total gamma flux to the ^{56}Fe inelastic, elastic and (n,γ) neutron cross sections for iron spheres with the radii of 12.5 and 17.5 cm.

neutron and gamma flux to the inelastic and elastic cross sections of ^{56}Fe.

The computational uncertainties due to iron nuclear data and the ^{252}Cf neutron and gamma source were studied using the new functionalities of the SUSD3D code. Depending on sphere radius, 20 to 50 % of gammas arriving in the detector corresponds to the prompt and delayed gammas emitted from the ^{252}Cf, which has relatively high uncertainty, contrary to the prompt neutron component which is a standard.

S/U studies confirm the high potention of the Iron sphere transmission experiment for nuclear data (ND) validation and verification (V&V) and reveal some specific features. Variing spheres radia provides a selective information on the relative impact of different ND reactions (elastic/inelastic) to neutron flux of different energies. It was found that the neutron flux below 1 MeV is relatively little sensitive to diameter variations for the Fe sphere diameter between 25 – 35 cm. On the other hand, variing the diameter largely impacts the sensitivity of high neutron enegy flux to iron elastic and inelastic cross sections, therefore trend analysis could provide information on ND deficiencies for the specific energy ranges and reactions.

Furthermore, sensitivity of the gamma flux to Fe elastic and inelastic cross sections change sign with increased iron sphere thickness, which could be exploited for the interpretation of the observed C/E trends and for guiding future nuclear data improvements.

KFK benchmark was performed 45 years ago and the measurements are in some aspects not sufficiently accurate to reliably concude on the quality of the modern ND evaluations and to guide the specific improvements. Repeating these measurements using modern measurement techniques is expected to be valuable for V&V purposes. ND S/U analyses could be valuable to assist in the design of the experimental configuration.

The uncertainties in the calculated gamma spectra can be only very partly estimated using the available neutron covariance data. A complete evaluation of gamma spectra uncertainties from the sensitivities will necessitate in addition to the neutron also gamma-ray covariance data, as well as the uncertainties in gamma emission spectra, ^{252}Cf prompt/delayed gamma source, secondary distributions etc., which are not yet available.

Declaration of competing interest

The authors declare that they have no known competing financial interests or personal relationships that could have appeared to influence the work reported in this paper.

Acknowledgments

This work has been partly funded by the RCUK Energy Programme [grant number EP/W006839/1]. To obtain further information on the data and models underlying this paper please contact PublicationsManager@ukaea.uk. Some fusion benchmark analyses were partly funded by the EUROfusion project within EC fusion programme (2024).

Data availability

The data will be made available on request. The sensitivities will be included in the SINBAD database.

References

R. E. Alcouffe, R.S. Baker, J.A. Dahl, S.A. Turner, R.C. Ward, PARTISN 5.97, 1-D, 2-D, 3-D Time-Dependent, Multigroup Deterministic Parallel Neutral Particle Transport Code, LA-UR-08-07258, NEA/Data Bank CCC-0760/01 computer code collection, November 2008.

D. Brown, et al., ENDF/BVIII. 0: the 8th major release of the nuclear reaction data library with CIELO-project cross sections, new standards and thermal scattering data. Nucl. Data Sheets **148**, 1 (2018).

Fusion Evaluated Nuclear Data Library - FENDL-3.2b, https://www-nds.iaea.org/fendl/.

S.-H. Jiang and H. Werle, "Measurement and calculation of ^{252}Cf-fission neutron induced gamma fields in iron", Report NEACRP-L-196(1977).

Jiang, S.-H., Werle, H., 1977. Messung und Berechnung der durch ^{252}Cf-Spaltneutronen in Eisen induzierten g-Felder. Report KFK-2444.

Jiang, S.-H., Werle, H., 1978. Measurement and Calculation of Californium-252 Fission Neutron-Induced Gamma Fields in Iron. Nucl. Sci. Eng. 66, 354.

Kodeli, I., 2001. Multidimensional Deterministic Nuclear Data Sensitivity and Uncertainty Code System: Method and Application. *Nucl. Sci. Eng.* 138, 45.

Kodeli, I., 2023. XSUN-2022/SUSD3D n/γ sensitivity-uncertainty code package with recent JEFF-3.3 and ENDF/B-VIII.0 covariance data. EPJ Web of Conferences 281, 00013. https://doi.org/10.1051/epjconf/202328100013.

Kodeli, I., et al., 2023. Outcomes of WPEC SG47 on "Use of Shielding Integral Benchmark Archive and Database for Nuclear Data Validation". EPJ Web of Conferences 284, 15002.

I. Kodeli, S. Slavič, "SUSD3D Computer Code as Part of the XSUN-2017 Windows Interface Environment for Deterministic Radiation Transport and Cross Section Sensitivity-Uncertainty Analysis," *Science and Technology of Nuclear Installations*, Volume **2017**, Article ID 1264736, (2017).

Kodeli, I., Sartori, E., 2021. SINBAD - Radiation Shielding Benchmarks Experiments. Ann. Nucl. Energy 159, 108254.

I. Kodeli, ANGELO-LAMBDA, Covariance matrix interpolation and mathematical verification, NEA-DB Computer Code Collection, NEA-1798/02 (2008).

R. E. MacFarlane, TRANSX 2.15, Code System to Produce Neutron, Photon, and Particle Transport Tables for Discrete-Ordinates and Diffusion Codes from Cross Sections in MATXS Format, RSICC Peripheral Shielding Routine Collection, PSR-317 (1995).

A.J.M. Plompen, O. Cabellos, C. De Saint Jean *et al.*, The joint evaluated fission and fusion nuclear data library, JEFF-3.3. *Eur. Phys. J. A* **56**, 181 (2020). https://doi.org/10.1140/epja/s10050-020-00141-9.

Simakov, S., 2024. Evaluation of the prompt γ-ray spectra from spontaneous fission of ^{252}Cf (No. Report INDC(NDS)-0887). International Atomic Energy Agency. Vienna. https://doi.org/10.61092/iaea.x6kd-w5qa.

S.P. Simakov, U. Fischer, Iron Sphere Benchmarks with ^{252}Cf source: IPPE cf. with KFK and NIST, Consultants' Meeting of International Nuclear Data Evaluation Network (INDEN) on the Evaluated Nuclear Data of the Structural Materials, 29 Oct - 1 Nov 2018, IAEA, Vienna.

S. Simakov, U. Fischer, KFK γ-ray leakage Iron sphere benchmark with Cf source: entry for SINBAD and analysis, KIT Scientific Working Papers 203 (Nov. 2022).

Werle, H., Bluhm, H., Fieg, G., Kappler, F., Kuhn, D., Lalovic, M., Oct 1975. Neutron Leakage Spectra from Iron Spheres with a Cf-252 Neutron Source in the Centre. Proc. of the Specialists' Meeting on Sensitivity Studies and Shielding Benchmarks, Paris.